

VMAP analytics

Smart Analytics for Multi-Scale Material and Manufacturing Modelling

Prevas use case – FEM analysis

Version	V1.1
Date	
Confidentiality	Public
Type of Deliverable	FE model and report
Description	Report
Deliverables in the Project	Deliverable D3.2a

Abstract

The project "VMAP analytics – Smart analytics for multi-scale material and manufacturing modeling" deals with digitalization, encapsulating the concept's essence. Various digital twins for various manufacturing processes are developed in this project. This report deals with the development of a 3D Finite Element model for a walking beam furnace at Outokumpu, Tornio. The 3D FEM model is developed in MATLAB to predict the evolution of skid marks. The heat exchange in the furnace is considered via a view factor that takes care of the obstructions in the furnace. The FEM results are validated with STEELTEMP via FOCS and found to be in good agreement. The 3D FEM developed in MATLAB provides additional information about the skid marks.

1. Change Log

2. Contributors:

Name	Organization
Johan Lindwall	Swerim

Table of Contents

PREVAS USE CASE – FEM ANALYSIS	1
1. INTRODUCTION	4
1.1. <i>Business Objective</i>	4
1.2. <i>Furnace description</i>	5
2. 3D FURNACE MODELLING.....	6
2.1. <i>Finite Element formulation</i>	7
2.2. <i>Boundary conditions</i>	9
2.3. <i>View factor interpolation</i>	12
3. SIMULATION METHODOLOGY	12
4. SIMULATION RESULTS	12
4.1. <i>Comparison to SteelTemp</i>	13
4.2. <i>Three-dimensional results</i>	14
4.3. <i>Effect of charging temperature</i>	15
5. CONCLUDING REMARKS	16

1. Introduction

Prevas provides advanced solutions and consultancy services within product development and production development. Prevas supply an unique solution: FOCS – Furnace Optimization Control System, to optimize furnace parameters. Today majority of all steel produced in Scandinavia is heated in a furnace controlled by FOCS. The primary goal of the FOCS is to minimize fuel consumption while simultaneously enhancing productivity and the quality of products in a range of furnace applications¹. These applications encompass pit furnaces, normalizing furnaces, annealing furnaces, and reheating furnaces. The temperature computation is executed through a 2D model known as STEELTEMP, which has been co-developed by MEFOS Swerim. The typical energy savings is in the range 5-20%. On top of reduced energy consumption, the system increases production capacity by intelligent pacing control of the furnace and surrounding processes. Productivity increases with up to 28% have been realized.

1.1. Business Objective

A reheat furnace is generally employed to bring slabs or metal workpieces to the proper temperature for hot rolling. Such furnaces normally include multiple zones and the heat is usually supplied from burners located above and below the slabs. The slabs are either pushed through the furnace on stationary, water cooled beams or moved from one end to the other using a combination of stationery and walking beams. Figure 1 shows the schematic picture of the furnace. The slabs are supported on skids which are cooled with water to prevent too rapid deterioration and to maintain the strength of the skids. This results in thermal gradients in the slab and continues to exist at the time of rolling, resulting in differences in the deformation resistance of the material and increasing the difficulty of rolling consistent gage metal. Figure 2 shows the skid marks developed in the slabs.

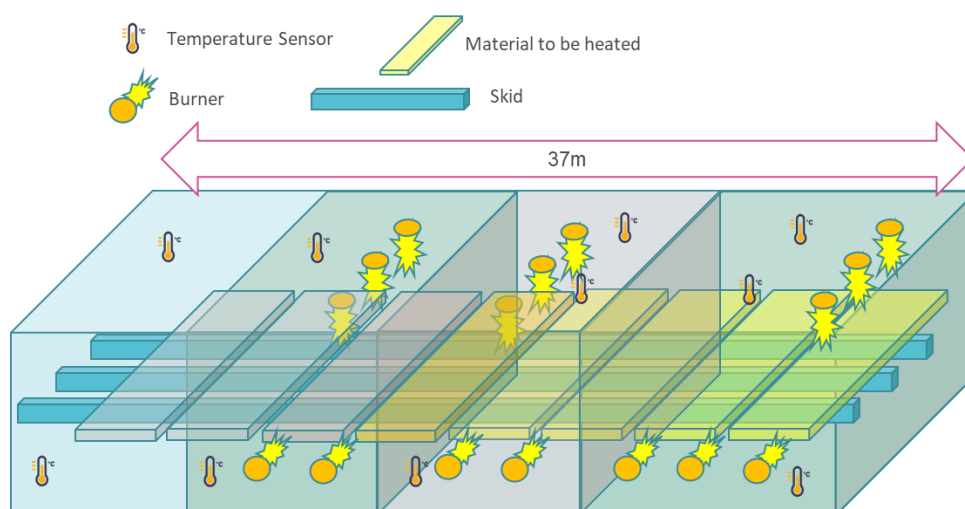


Figure 1 The schematic picture of the furnace with different heating zones

¹ M Evestedt and P-O Norberg, Precise temperature control in high quality steel reheating and annealing furnaces, 13th Symposium on automation in mining, mineral and metal processing, Cape Town, South Africa, August 2-4, 2010.

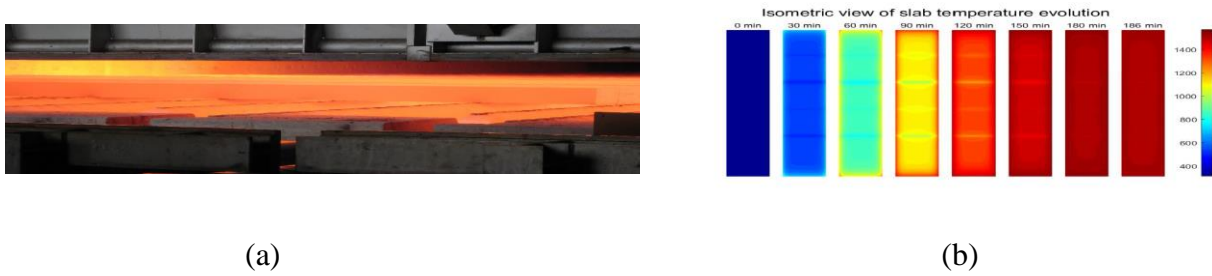


Figure 2 a) Slabs placed on water cooled skids and b) Evolution of skid marks in the furnace¹

These skid marks create inhomogeneous deformation and result in non-uniform thickness which are not desirable. Further, they affect the roll pass schedule. The main objective of the project is to develop a thermal FEA model to predict and understand the formation of skid marks.

1.2. Furnace description

Two walking beam furnaces are in use at the Outokumpu Hot rolling mill in Tornio, Finland. Slabs from melting shop are heated in a furnace before rolling. Weight of the slabs is approx. 23 tons. Carbon monoxide and natural gas are used as fuels in the furnaces and combustion air is heated in recuperators. Figure 3 shows Walking beam furnace 2 (WBF2). The effective length is 35.5 m. Charging takes place with the help of a long charger. The slabs can be placed in the furnace without large gaps if the arrival of the slabs is delayed.

The walking beams are electromechanically movable, the forward movement is 580 mm in WBF2. There are 7 fixed beams and 6 moving beams. The furnace has three zones, and the burners are located on the side of the furnace and there is a total of 72 of them. The discharging temperature varies between 1100 °C and 1250 °C. Skid marks are first noticed after heating as peaks in the rolling forces. Because the skid marks are colder areas, the material becomes more resistant to deformations, hence, they increase the rolling forces.

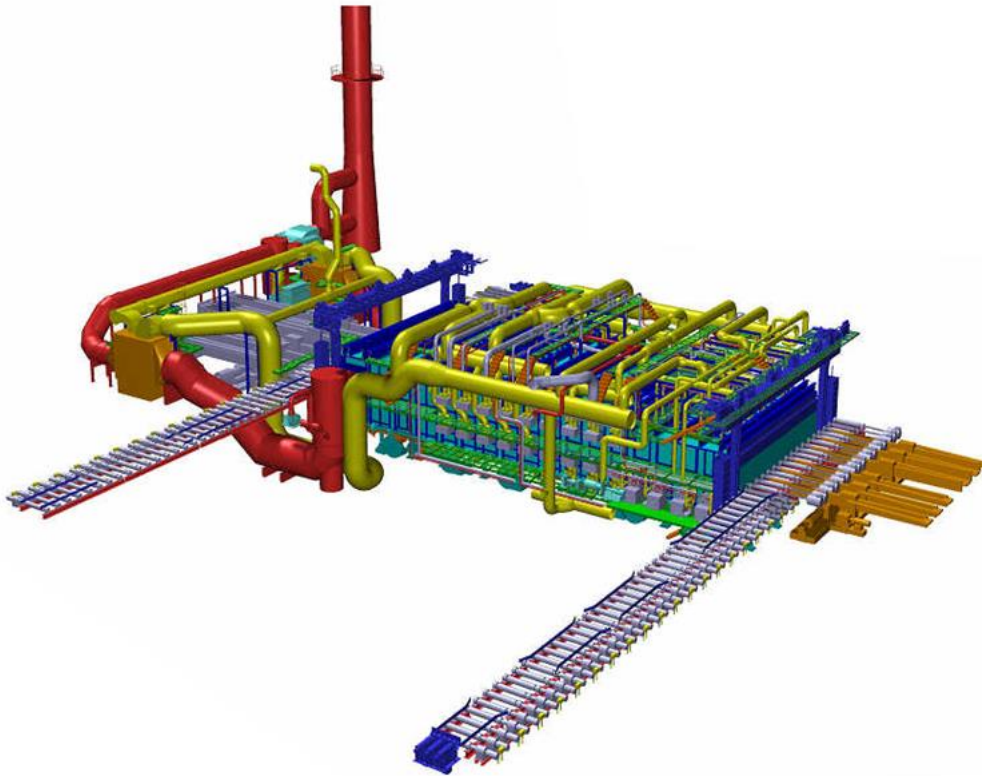


Figure 3 Schematic of the waling beam furnace 2 at Tornio (courtesy Outokumpu AB, Tornio)

2. 3D furnace modelling

Modelling of a walking beam furnace in three dimensions enables simulation of the complete temperature profile of the slab as well as the skid marks that results from the contact with the water-cooled beams. In a two-dimensional model, a cross section only be computed that is either parallel or perpendicular to the beams as illustrated in Figure 4.

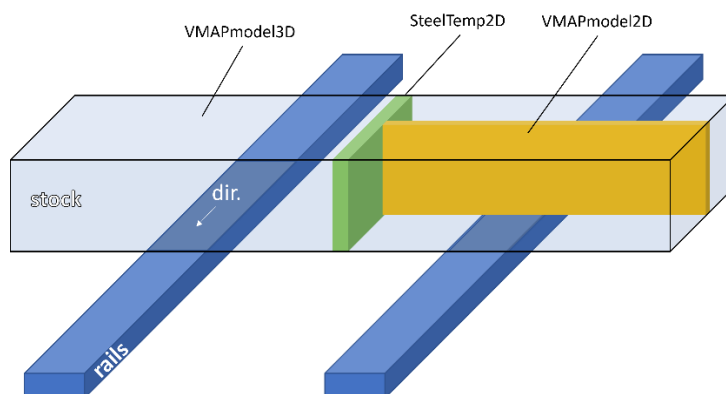


Figure 4 Modelling strategies in two and three dimensions.

The benefit of using a three-dimensional is that it can provide a complete representation of the temperature distribution, however, it will always be associated with higher computational cost and longer simulation times. The benefit with two-dimensional models is increased computational speed, even with higher spatial resolution. The modelling approach developed

in this task enables simulation in either two or three dimensions using Finite Element Analysis (FEA) as described in detail in the following sections.

2.1. Finite Element formulation

Finite Element Analysis (FEA) is a technique to compute a response of a system by a set of external and internal loads by dividing the domain into small subdomains, which are referred to as elements. Each element describes a set of equations which are solved at once in a global set of equations. The Finite Element Method (FEM) is the strategy used in the developed mode to calculate the temperature all instances simultaneously by numerical integration. The method includes the use of shape functions to describe the interaction of each element and to enable interpolation of the result of any position in space.

Two-dimensional linear shape functions

The linear shell element used in the 2D model are shown in Figure 5 with the positions of internal nodes 1-4 in each corner. The shape functions, N are used to describe the temperature within the finite elements by linear interpolation on the nodal values. The shape functions are described by $N_{1-4} = \frac{1}{4}(1 \pm r)(1 \pm s)$ and the span of the elements in the natural coordinate system (r - s) are $[-1,1]$. Linear interpolation within the element is done with integration points located at:

$$\begin{bmatrix} r \\ s \end{bmatrix} = \frac{1}{\sqrt{3}} \begin{bmatrix} -1 & 1 & 1 & -1 \\ -1 & -1 & 1 & 1 \end{bmatrix}. \quad (1)$$

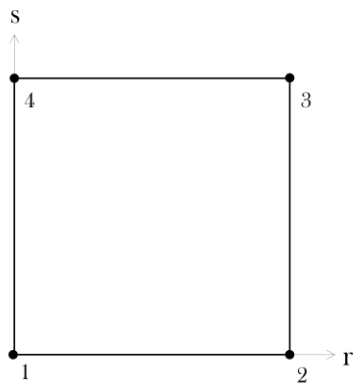


Figure 5 Linear 2D shell elements in the natural coordinate system (r - s (equivalent to x - y as no rotation is considered)).

Three-dimensional linear shape functions

The 3D elements used in the model uses eight nodes as shown in Figure 6 with local node numbering 1-8 in each corner. The shape functions in three dimensions are a natural expansion of the two-dimensional elements, now with shape functions $N_{1-8} = \frac{1}{8}(1 \pm r)(1 \pm s)(1 \pm t)$. Interpolation of the solution within the element is performed with the integration points at:

$$\begin{bmatrix} r \\ s \\ t \end{bmatrix} = \frac{1}{\sqrt{3}} \begin{bmatrix} -1 & 1 & 1 & -1 & -1 & 1 & 1 & -1 \\ -1 & -1 & 1 & 1 & -1 & -1 & 1 & 1 \\ -1 & -1 & -1 & -1 & 1 & 1 & 1 & 1 \end{bmatrix}. \quad (2)$$

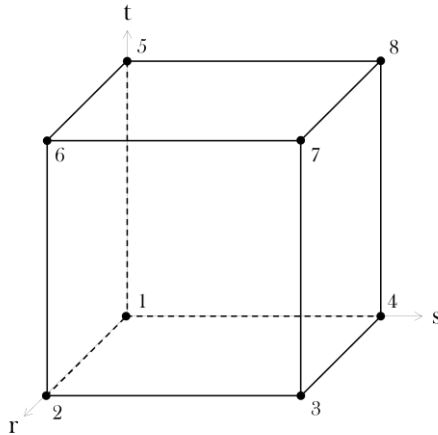


Figure 6 Linear 3D brick elements in the natural coordinate system (r-s-t) (equivalent to x-y-z as no rotation is considered).

Transient heat conduction

The heat flow in any isotropic medium can be described by the heat equation given as:

$$\rho c_p \frac{\partial T}{\partial t} - \nabla(k\nabla T) = \dot{q}_v \quad (3)$$

Where ρ , c_p and k are the material parameters: density (kg/m^3), specific heat capacity (J/kgK) and thermal conductivity (W/mK) respectively. The temperature, T is the unknown parameter and changes over time, t . The term \dot{q}_v describes the change in total thermal energy for the system over time. In terms of furnace reheating of a slab, this term contains the provided energy from the burning fuel via thermal flux at the slab surfaces, modelled with the boundary conditions described later.

Galerkin method

The temperature is the unknown in the thermal FEA and is computed in all nodal positions of all elements. The temperature is approximated by minimizing the weight functions, W for each position in time and space:

$$T(x, y, z, t) = \sum_i W(x, y, z)_i T_i(t) \quad (4)$$

The solution of $T(x, y, z, t)$ can be found by integration of parts of the right-hand side. This is leading to a spatial solution of the transient heat conduction equation where it is written on weak form using the shape function as the weighted function. The solution can then be approximated in the time space with finite difference for all finite elements in the spatial domain. The resulting solution of the transient heat conduction in all elements, m can be compressed in the following matrix form.

$$\mathbf{M} \frac{d\mathbf{T}}{dt} + \mathbf{K}\mathbf{T} = \mathbf{f} \quad (5)$$

Explanation of each component follows below. First is \mathbf{M} which represents the global heat capacity matrix with the temperature dependent material properties as mentioned previously:

$$\mathbf{M} = \sum^m \int_V \rho c_p N N^T dV \quad (6)$$

Note that the shape functions are element type specific, meaning that the same numerical strategy is used in both 2D and 3D. The only difference between the addition of one dimension is the size of the matrices as N increases in size. The global matrix is constructed by summing the contribution of each node associated with all finite elements where all nodes have unique numbers, ranging from one to the total amount. Thus, the global matrix will have the size $[n \times n]$ where n is the total number of nodes in the system. The second term in equation (5) includes \mathbf{K} which represents the global conductivity matrix:

$$\mathbf{K} = \sum^m \int_V k \nabla N \nabla N^T dV. \quad (7)$$

Here ∇ operates on the natural coordinate system of the finite elements, whenever it is in 2D or 3D. The assembly of \mathbf{K} is done by the same approach as \mathbf{M} . The final term in equation (5) is the source vector, \mathbf{f} containing the internal and external heat fluxes Q and q respectively:

$$\mathbf{f} = \int_V N Q dV - \int_{\Omega} N q d\Omega \quad (8)$$

The first term is the volumetric heat flux caused by internal or external heating/cooling. The term Q can for example represent latent heat of transformation that is independent on the surrounding temperature. The second term includes the heat exchange with the surroundings on the boundary element faces. The term q includes the heat flow by convection and radiation which is driving the material heating in a furnace. This is therefore a very important parameter and the way it is modelled is described in the following sections.

2.2. Boundary conditions

The boundary conditions during external heating can also be described as heat input models. The heat input models will be responsible for the change in total thermal energy in the slab over time. The remaining components will be responsible for thermal energy re-distribution within the slab.

Convective heating

Convective heat transfer describes the heat flux over the boundary element faces when the solid material and the ambient temperature, T_a is unequal. The heat flux in the normal direction of the boundary elements is described by:

$$q = \alpha T - T a \quad (9)$$

where α is the convective heat transfer coefficient (W/mK). The convective heat transfer contributes both to the source vector \mathbf{f} and the conductivity matrix \mathbf{K} .

$$\mathbf{f} = \int_{\Omega} N \alpha T_a d\Omega \quad (10)$$

$$\mathbf{K} = \mathbf{K} + \int_{\Omega} N N^T \alpha d\Omega \quad (11)$$

$d\Omega$ represents the side length or area of each boundary element in 2D or 3D respectively. Thus, this additional term affects the external source term as well as the heat conductivity due to the imposed thermal gradient according to Fick's law.

Radiative heating

All mediums with a temperature radiate heat flux by $\varepsilon \sigma T^4$. Where ε is the emissivity factor and $\sigma = 5.67 \times 10^{-8}$ (W/m²K⁴) is the Boltzmann's constant. The surface also absorbs radiative heat from surrounding surfaces that radiates so that the net flux can be described as:

$$q = \frac{R\sigma}{\frac{1}{\varepsilon_s} + \frac{1}{\varepsilon_w} - 1} (T_w^4 - T_s^4) \quad (12)$$

where index s and w represent the surface of the slab and the walls in the surroundings respectively. Heat exchange via thermal radiation is limited whenever two surfaces of finite size are non-parallel or partly visible to one another. This reduction of potential heat exchange is modelled by multiplying a view factor/configuration factor R to the radiation heat flux equation. The view factor can take any value between zero and one where zero gives no heat exchange and one represent the theoretical highest heat exchange, equivalent to two parallel surfaces with infinite size. A geometric relation between two arbitrary surfaces is shown in Figure 7 and the view factor on surface 1 by surface 2 can be described according to² as:

$$dR_{1-2} = \frac{\cos \theta_1 \cos \theta_2}{\pi S^2} dA_2. \quad (13)$$

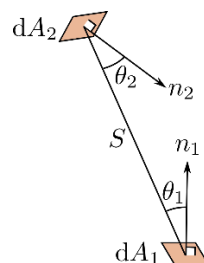


Figure 7 Two planes and the relations to define the view factor.

² Concepts and applications of finite element analysis. John Wiley & Sons, 2002.

In the FEA, dR is computed at each boundary element by summing the contribution from all wall segments in the furnace. The angles are determined by the scalar product of the vector s , which is the distance between the planes, and n , which are the normal vectors of each plane. Whenever Θ_1 or Θ_2 is greater than π , the contribution by dA_2 is set to zero because then the surfaces are faced away from each other. Sometimes, two planes that are faced toward each other are intersected by other wall segments. Therefore, the developed model includes automatic detection of shadowing planes and the correlating view factor is then set to zero. Figure 8 shows an example of three stock positions in a fictive furnace where some walls are shadowing the heat exchange between the furnace walls and the stock.

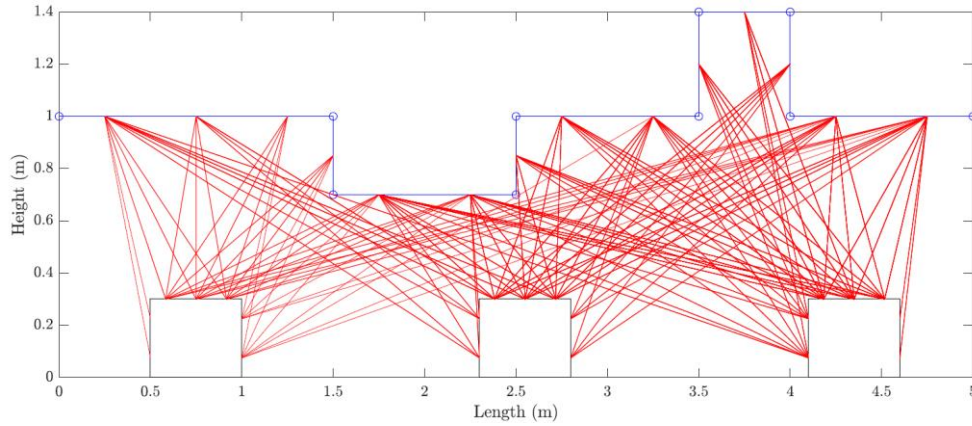


Figure 8 Illustration of discretized radiative heat exchange (red lines) between furnace walls and stock at three positions in a fictive furnace.

The contribution by thermal radiation is added to the FEA by rewriting of Equation (12) by factorization to match the construction of the convective heat flux in Equation (9). This simplification makes it possible to express the contribution from radiative heating as

$$q = h_{rad}(T_w - T_s) \quad (14)$$

and will have the same form as the convective heat flux. The introduced term h_{rad} has the same properties as the convective heat transfer coefficient and is computed as

$$h_{rad} = \frac{R\sigma}{\frac{1}{\varepsilon_s} + \frac{1}{\varepsilon_w} - 1} (T_w^2 + T_s^2)(T_w + T_s) \quad (15)$$

Finally, the contribution by radiation is added by substituting the convective heat transfer coefficient in Equations (10) and (11) by an effective heat transfer coefficient given by

$$\alpha_{eff} = \alpha + h_{rad}. \quad (16)$$

This method results in that the solution becomes highly non-linear, as the coefficient depends to the power of four on the unknown temperature at T_s . This motivates the use of an iterative implicit solver to minimize the residual of Equation (5) when the global matrices are constructed. For this is a Newton-Raphson iteration scheme used and the solution in every time increment is only accepted when converged to a given tolerance.

Thermal contact

Thermal contact is not modelled in this work. It would, in fact, be relatively straight forward to add the contribution to the effective heat convection coefficient. However, this would require some calibration and additional assumptions.

2.3. View factor interpolation

The calculations of view factor in the three-dimensional model are significantly time consuming due to the large amount of boundary elements. Therefore, a method was developed to pre-compute the spatial view factor as a geometrical factor in a fine mesh grid within the furnace. This makes it possible to, instead of computing the view factor at every finite element, interpolate the equivalent view factor in the pre-compiled data base. The simulation speed up is enormous by this approach with very little effect on the result. One caveat with this approach is that the view factor is not truly a geometrical factor.

3. Simulation methodology

The simulation methodology includes solving the heat conduction equation (5). This is done in an iterative approach as the solution is highly non-linear due to radiative heating, and solution depends on the unknown temperature to the power of four. A calculated temperature will be tested by moving all terms to one side in the equation, resulting in a residual, \mathbf{R} . The residual indicates how well the solution predicts the unknown temperature.

$$\mathbf{R} = \mathbf{M} \frac{d\mathbf{T}}{dt} + \mathbf{K}\mathbf{T} - \mathbf{f} \quad (17)$$

The first attempt is done with an initial guess of the unknown temperature, which is simply set as the previous temperature. Thus, $d\mathbf{T}$ will be zero in the first computation and the heat capacity matrix, \mathbf{M} will have no effect to the solution. After the first residual has been computed, the new temperature is computed by letting $d\mathbf{T}$ and \mathbf{T} contain the unknown temperature and the previous guess, i.e. $d\mathbf{T}=(\mathbf{T}_{\text{new}} - \mathbf{T}_{\text{old}})$ and $\mathbf{T}=\mathbf{T}_{\text{new}}$. Thus, the solution of \mathbf{T} requires inverse multiplication with $\text{inv}(\mathbf{M} / dt + \mathbf{K})$ which is the most time consuming operation in the solution strategy. The procedure is continued until the temperature change between two iterations is below a convergence criterion, usually set to $|d\mathbf{T}|/|\mathbf{T}| < 10^{-4}$. The assembly of the matrixes is redone between each iteration to reach a accepted solution with material properties and boundary conditions evaluated at the updated temperature. When a solution is accepted can a new time increment be evaluated where the boundary conditions and stock position in the furnace are updated according to the procedure presented in Section 3.2.

4. Simulation results

The developed code was initially tested by letting a square steel plate with a uniform initial temperature be heated by an ambient temperature from one side. The higher temperature from the surrounding was heating the material by convection and the thermal energy was transferred to the material by conduction as shown in Figure 9. The resulting temperature at three control points (left, center and right side) was compared to the results obtained by the commercially available FE-software LS-Dyna with identical setup and material data. As can be seen in the plot in **Error! Reference source not found.** 9, the results are identical.

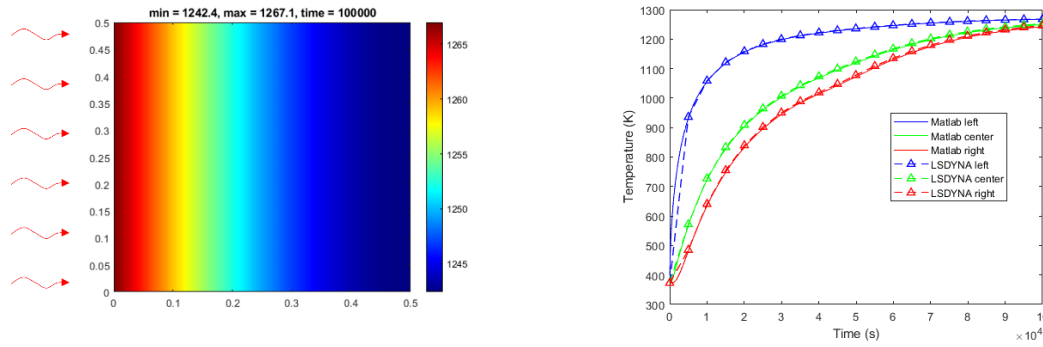


Figure 9 Benchmarking of the developed code with the commercial software LS-Dyna shows identical results.

4.1. Comparison to SteelTemp

The calculated temperature evolution in the slabs was compared to real time data gathered at Outokumpu in Tornio by Prevas. The data is the result of the temperature calculations provided by the FOCS-system. FOCS uses SteelTemp to compute the temperature in the material based on the measured temperatures at the furnace walls. The results are related to the position in the furnace and can vary depending on the operational conditions. Figure 10 shows the position of the stock versus the time in the furnace. It can be clearly seen that the forward motion is not linear as it would be in a theoretical ideal case. In Figure 10b a stop is clearly seen as the material stays for a about 50 minutes at the same position at 28 m. A simulation that followed the dashed line would in case b cause an under prediction of the heat input as the stop occurs at a relative hot position in the furnace.

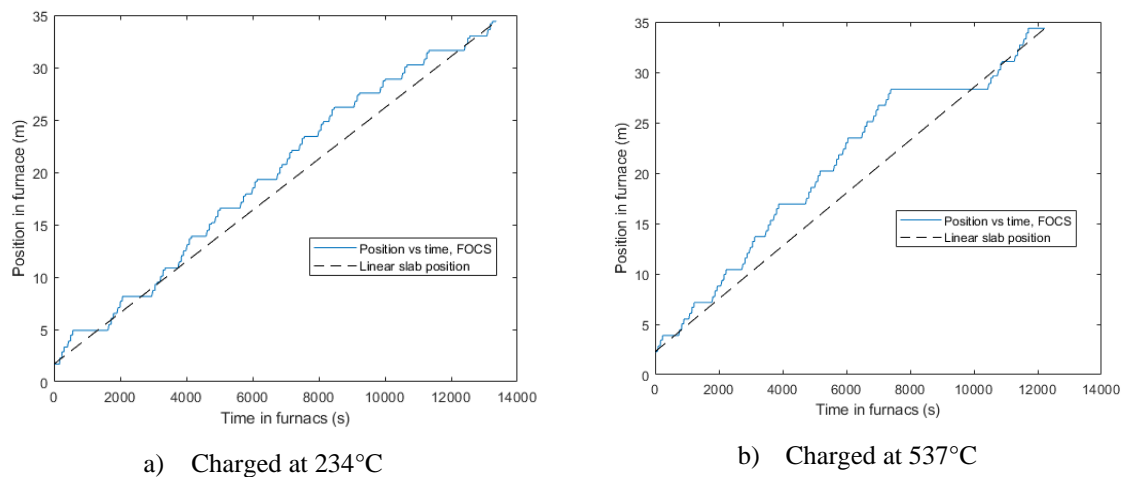


Figure 10. Position of stock versus the time in furnace.

It is necessary to use the same position vs time data for the stock in the simulations to obtain comparable results from the FOCS. Thus, the position vs time data was used directly to overwrite the linear forward motion of the stock. The results from the simulations are shown in Figure 11 with two different charging temperatures, 234°C and 537°C. The elapsed simulation time was about 2 seconds in each case using a mesh resolution of 20x15x2 nodes in height, width, and length respectively. Thus, the calculations were performed in three

dimensions, but the length of the slab is reduced to the minimum of only one element to replicate the computational domain used in SteelTemp.

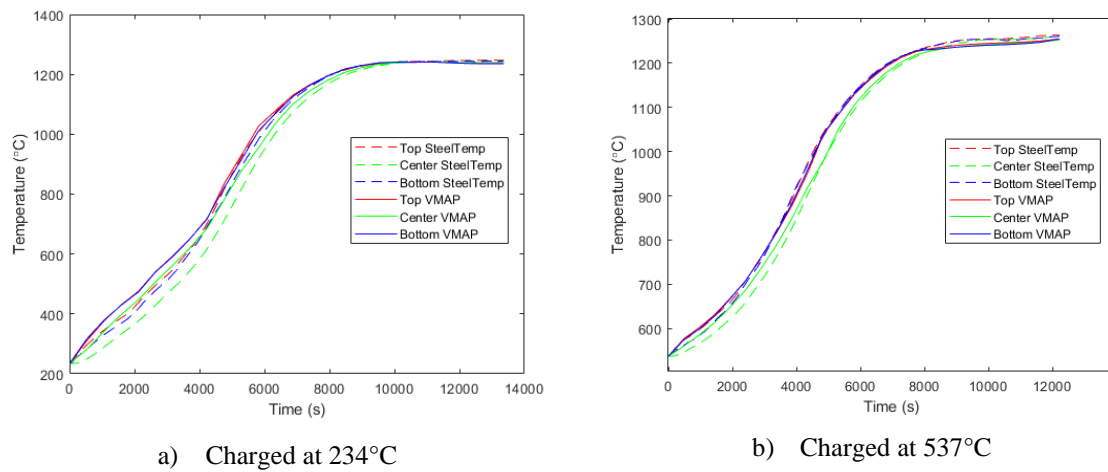


Figure 11. Temperature calculations in slab during different charging conditions.

As can be seen from the figures, the results are very similar even though the modelling procedure have some differences. The model developed in VMAP takes no consideration of the gas interaction, but it uses the predicted temperature as an input for the heat convection. The developed model also uses fixed values for the convection heat transfer coefficient ($80 \text{ W/m}^2\text{K}$) and the emissivity of the wall and slab (0.9 and 0.8 respectively). In SteelTemp on the other hand, these values can vary with the temperature.

4.2. Three-dimensional results

The simulations were also extended to the full length of the slab, including the moving and static beams. Because of symmetrical conditions, only half of the slab length was modelled. Due to the lack of calibration, direct heat loss to the water-cooled beams was not considered. Only the shadowing effect by the presence of the geometry was modelled. Hence, the view factor was set to zero at the locations of the static beams, and 0.2 at the locations of the moving beams as these are lower than the stock. The value 0.2 was arbitrary chosen due to simplicity.

The resulting temperature can be post processed in any time instance and position of the slab as presented in Figure 12. The skid marks are clearly seen on the top surface as stripes with lower temperatures. The static beams are more pronounced than the moving beams as expected.

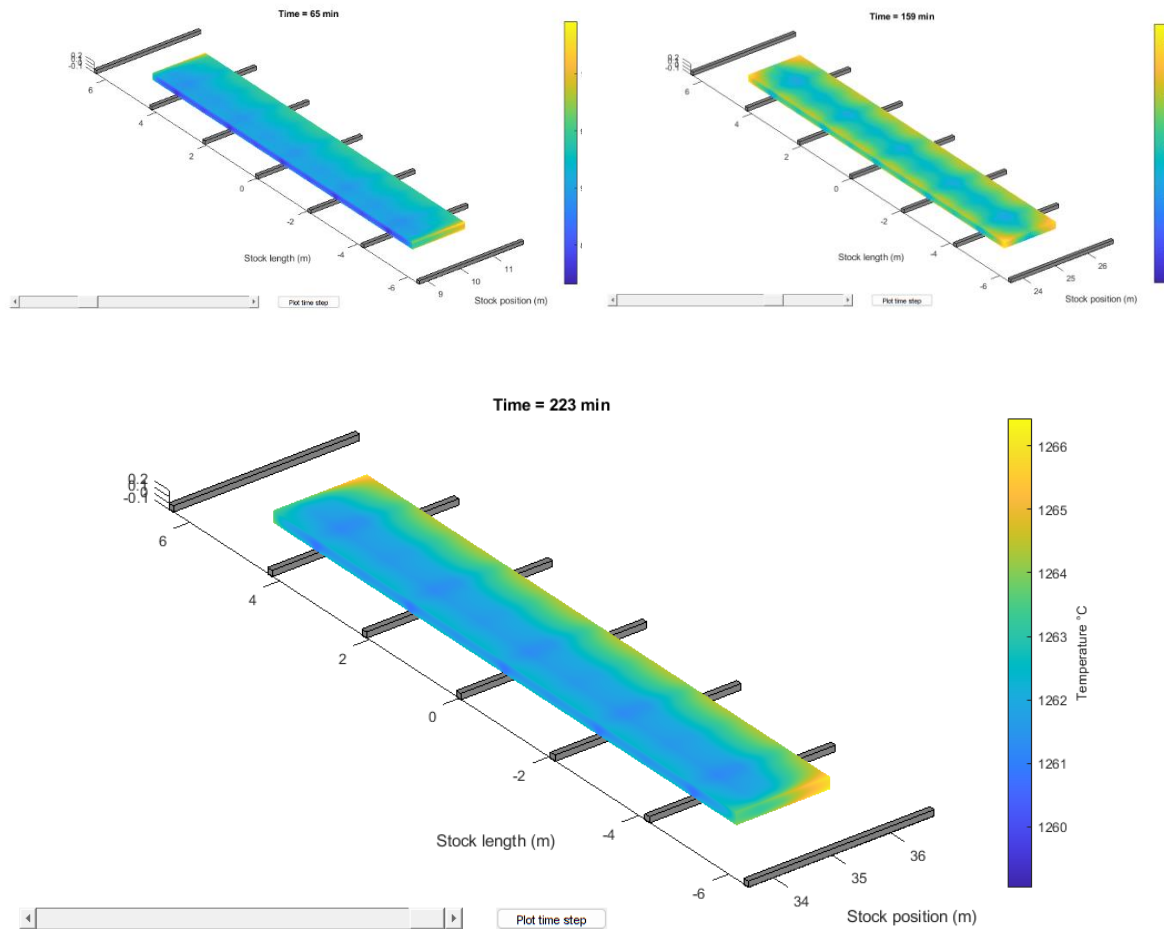


Figure 12. Temperature distribution in 3D computed with the developed FE-model in MATLAB at different position in furnace with effect of moving and static beams.

The simulation time with the true three-dimensional models were 44 s and 38 s respectively for the material charged at 234°C and 537°C. The difference in simulation time is due to the different dimensions of the two materials. The colder charges material was 11.511×1.286×0.202 m (length, width, and height) whereas the hotter charged material was 10.305×1.592×0.202 m. The mesh resolution in the length direction was 47.62 mm, resulting in 121 and 109 nodes in each case.

4.3. Effect of charging temperature

During the final stage of the heating operation, some interesting things are taking place. The last zone of the furnace is the soaking zone. In the soaking zone is the temperature meant to equalize to reduce the temperature gradients in the material. Up to this point, the core of the material has been consistently colder than the surfaces because of the heating from the surroundings. In the soaking zone the temperature will be lower than in the heating zones, and occasionally also lower than the surface temperature of the stock. This means that the surface temperature may drop while the core temperature continues to rise. The time spent in the soaking zone is beneficial for reducing the skidmarks, as more time is given for thermal diffusion. When looking at the heating curves in Figure 11 11a, it can be seen that a relatively long time is spent in the soaking zone. Thus, the skid marks can be expected to reduce, especially from the top side. This is in fact what can be seen in the simulations, in

Error! Reference source not found.3a. The temperature variations at the top surface and center is expected to vary very little. In the other case, Figure 1111b, the temperature continues to increase due to the quick finish and the core temperature never equalizes. Thus, the skid marks will remain on the finished product according to the results in Figure 13b.

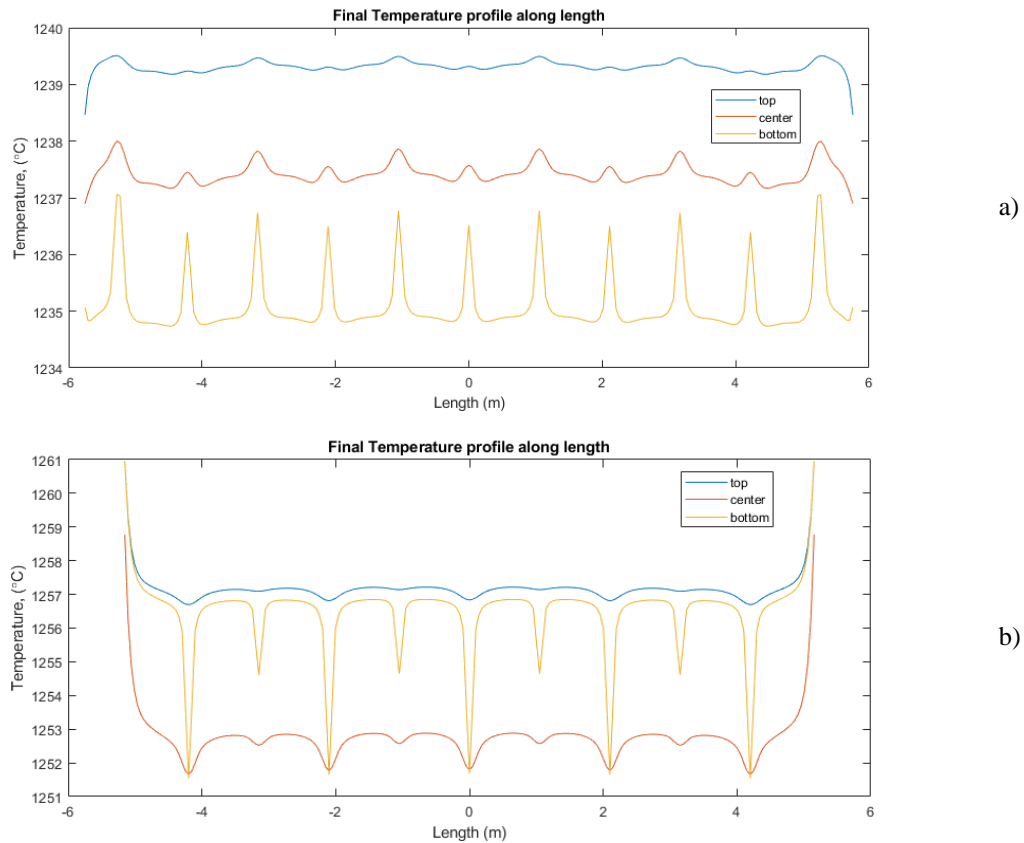


Figure 13. Final temperature profile along the slab length at charging at a) 234°C and b) 537°C.

The results require an important explanation and perhaps a warning. The skid marks are only modelled by limiting the heat input from convection and thermal radiation. If the case is as in **Error! Reference source not found.**2a, the assumption will only act as an isolation such that no heat is radiating out from the material to the colder surroundings. Therefore, the skid marks at the bottom surface can appear as high temperature peaks. The reality is that heat is conducted through the contact area, so this scenario would most likely not happen in reality. However, the lack of heat loss in the contact area is covered up by the assumption if the material undergoes heating. Calibration of the heat loss through the contact to the beams are necessary for more accurate results; however, this is a challenging task.

5. Concluding remarks

The simulation result by the developed FE-model in MATLAB is highly accurate as compared to the predictions by SteelTemp via FOCS. The modelling approach involves some simplifications that may influence the predictions. On major simplification is that the combustion gas is not considered during the radiative heating. It is well known that the gas can both absorb and emit thermal energy. However, the effect of ignoring this effect is not significant when the results are compared with FOCS. Another simplification is that heat loss

to the surrounding is not considered. However, this will have no effect on the results as the wall temperature is set based on the data provided by FOCS.